The JPL Optical Communications Telescope Laboratory Test Bed for the Future Optical Deep Space Network

K. E. Wilson,[1] N. Page,[2] J. Wu,[1] and M. Srinivasan[1]

The lower power consumption and lower mass of high-bandwidth optical telecommunications relative to RF telecommunications make laser communication technology extremely attractive for returning data from future NASA/JPL deep-space probes. JPL is building a research and development optical communications telescope laboratory (OCTL) at its Table Mountain Facility in Southern California to evaluate strategies for supporting operations from future deep-space optical links. The telescope is scheduled for delivery in the spring of 2003, and among its early experiments will be the use of retroreflector-bearing satellites to assess multiple-beam strategies to mitigate the effects of atmospheric scintillation on the uplink. Designed to be an optical antenna for both daytime and nighttime communications, the OCTL will be a test bed for evaluating strategies to support communications at small Sun–Earth–probe angles.

I. Introduction

NASA has recently announced plans to demonstrate an optical communications link from Mars to Earth. The optical terminal will be on the Mars Telesat [1] that is scheduled for launch in 2009 [1]. Studies currently are under way to define the details of the demonstration. However, initial goals call for demonstrating data rates of 10 Mb/s at conjunction (∼2.37 AU at 2011) and 100 Mb/s at opposition (∼0.67 AU at 2011), rates that are far in excess of those achieved by RF systems.

Historically, JPL has been responsible for technology development for NASA's Deep Space Network (DSN). To support future deep-space optical links, JPL plans to perform a series of technology demonstrations that will extend from the development of acquisition and tracking approaches using its deep-space terminal concept [2] to the investigation of the effects of cloud cover on the availability of the optical channel [3]. With the completion of its Optical Communications Telescope Laboratory (OCTL), JPL will begin to develop operational strategies and procedures for the future Optical Deep Space Network (ODSN).

---

[1] Communications Systems and Research Section.

[2] Interferometry Systems and Large Optical Systems Section.

The research described in this publication was carried out by the Jet Propulsion Laboratory, California Institute of Technology, under a contract with the National Aeronautics and Space Administration.

Past research has shown that acquisition, tracking, and pointing of an optical terminal onboard a spacecraft at Mars can be accomplished by using a combination of uplink laser beacon and inertial sensors [4]. Strategies using multi-beam uplinks, with seeing-limited beam divergence to mitigate atmospheric scintillation, limit the applicability of the laser-beacon approach to a distance of approximately 1.5 AU. Beyond this range, one needs to compensate for atmospheric turbulence. Adaptive optics techniques can realize near-diffraction-limited (dl) beam divergences from the uplink aperture and as much as a $(\Theta_{sl}/\Theta_{dl})^2$ gain over atmospheric seeing-limited (sl) divergence.

In this article, we describe plans for some of the future research to be done at the OCTL. In the following section, we describe the design specifications of the OCTL telescope. Next we discuss planned beam-propagation experiments and the optical-train design for high-power laser beam propagation from the OCTL. This discussion is followed by the results of our preliminary analysis on the benefits of adaptive optics to deep-space communications in the presence of sky background noise. Finally, we describe a multi-tiered beam propagation safety zone, its integration into the OCTL, and strategies for safe laser beam propagation through these tiers. The process described here is seen as an essential precursor to unattended autonomous laser beam propagation from remote sites.

II. The OCTL Telescope

The OCTL building is shown in Fig. 1. The dome is equipped with an air-handling system that controls its temperature to within 5 deg of the external temperature when the telescope is not in operation. This system reduces the differential temperature between the dome and the outside air and alleviates the effects of dome seeing when the telescope is opened for operation. The telescope is a coudé focus instrument with an elevation/azimuth (El/Az) mount. The telescope is supported on an open-structure pier that allows free air exchange within the coudé room. A transparent window of BK-7 glass thermally isolates the optical path between the coudé room and the dome. The window is kept dust-free by a continuous flow of dry nitrogen across its face. During operations, thermal effects in the telescope observation path are reduced by venting the heat generated by the laser in the coudé room and by locating personnel approximately 30-m downwind of the telescope.

Figure 2 shows the telescope undergoing tests at the vendor's (Brashear LP) Pittsburgh, Pennsylvania, facility. The telescope has a 1-m aperture and an f/75.8 coudé focus to support high-power laser beam propagation. Telescope specifications call for an optical figure of 0.054λ rms wave-front error at a test wavelength of 0.633 μm. The telescope is supported on an El/Az mount and will track objects from low Earth orbit (LEO) (250 km) to deep-space ranges. The tracking specifications are given in Table 1.

Fig. 1. The OCTL telescope building and dome at Table Mountain Facility in Wrightwood, California.

Fig. 2. The OCTL telescope undergoing testing at the vendor's facility. The louvered baffles, the 20-cm acquisition telescope, and the M4 and M5 coudé path tube are shown.

Table 1. OCTL telescope tracking performance requirements.

Characteristic	Azimuth	Elevation
Travel	±335 deg	−5 to +185 deg
Maximum rate	20 deg/s	5 deg/s
Maximum acceleration	10 deg/s^2	5 deg/s^2
Frequency band	0.1 to 20 Hz	20 to 1000 Hz
Tracking rate, required LOS jitter		
$0.007 < d\Theta/dt < 0.54$ deg/s	<10 μrad (2 μrad desired)	<1 μrad
$0.5 < d\Theta/dt < 2$ deg/s	<10 μrad	<1 μrad

Designed as an optical antenna, the telescope will operate during the night and in the day as close as 30 deg of the Sun. It will operate in winds up to 50 km per hour and with temperatures rangingfrom −10 deg C to 40 deg C. To meet the thermal requirements, the telescope mirrors M1 through M7 are made of zerodur, with M1 through M3 enclosed in louvers. A system of fans maintains a flow of air across the primary mirror. When operating at greater than 30 deg to the Sun, the design calls for a minimum of 65 percent of the received energy to be enclosed in the first Airy disk (1.54-μrad diameter) and 83 percent to be enclosed in the first Airy disk and first ring (2.81-μrad diameter). To allow testing to the limits of the system's performance, the telescope operator will be able to replace the standard secondary mirror spider-support heat shields with wider ones that will protect the mirror support when the telescope is pointed between 10 deg and 30 deg of the Sun. With the wider heat shields in place, the encircled energy drops to 61 percent and 80 percent in the first Airy disk and in the first Airy disk plus first ring, respectively.

The performance specification for pointing at 30 deg to the Sun calls for the light scattered in a 100-μrad-square field of view to be less than 20 pW/Å over the 5,000 to 20,000-Å spectral range, with less than 10 pW/Å at 10,642 Å. To meet the scattered light specification, the louvers were painted white on the outside to reduce heat loading on the structure and black on the inside to reduce the light scatter from mounting surfaces. Daytime operation will allow future development of background rejection and scintillation-mitigation strategies.

To meet the requirement for a high-efficiency telescope over the 0.5-μm to 2.0-μm operational wavelength band, we took advantage of the dry Southern California climate and selected a silver coating for its high reflectivity. All seven mirrors were coated with Denton FSS-99 protected silver to achieve the maximum optical transmission in the visible and near-IR.

III. Planned OCTL Experiments

OCTL experiments planned over the next 5 years include the following:

(1) Multi-beam propagation

(2) Development of strategies for safe laser beam propagation

(3) Development of autonomous telescope operation strategies

(4) Development of adaptive optics capability to reduce sky background noise

(5) Demonstration of air-to-ground optical links

(6) Demonstration of optical communications with other targets of opportunity

While multi-beam strategies mitigate the effects of atmospheric scintillation on the uplink beam, adaptive optics can reduce the effects of atmospheric scintillation on both the uplink and downlink beams. On the uplink, adaptive optics compensation for atmospheric turbulence enables propagating narrow beams to the spacecraft. On the downlink, reducing the ground receiver's field of view (FOV) can enhance the signal-to-noise ratio (SNR) when pointing close to the Sun. The planned adaptive optics experiments will explore techniques to mitigate both of these effects.

IV. Optical Train Design for Active Satellite-Tracking Experiments

The targets for beam propagation experiments will be Earth-orbiting, retroreflector-bearing satellites that range in altitude from 700 km to 19,000 km. JPL has registered with the National Space Development Agency of Japan, and has received permission to illuminate Laser Ranging Equipment (LRE) and Ajisai. Target satellites will be illuminated with the pulsed Nd:YAG laser shown in Fig. 3; its operating characteristics are given in Table 2. The laser's repetition rate has been modified from a fixed 50 Hz to one that is selectable between 1 and 50 Hz. This variable repetition rate allows combining time-division multiplexing and polarization isolation to achieve transmit/receive isolation. To maintain the thermal loading of the cavity and ensure that the beam quality and divergence are unchanged at the various repetition rates, the flash lamps are operated at rates of 48, 49, or 50 Hz while the Q-switch is triggered

Fig. 3. Picture of a Q-switched Nd:YAG laser beam. The laser operates at a variety of pulse-repetition rates between 1 and 50 Hz.

Table 2. OCTL Nd:YAG laser beam characteristics.

Parameter	0.532 μm	1.064 μm
Beam diameter at exit		
Vertical, mm	11.5	11.5
Horizontal, mm	7.4	7.4
Mean pulse width, ns	6.6	8
Standard deviation, ps	219.9	151.9
Pulse jitter, ns	2.7	2.1
Average power, W	12.8	29.7
Energy per pulse, J	0.25	0.6
Power stability (%), 1 s	5	6.5
Beam divergence, mrad	0.49	1.0
Polarization extinction ratio	5.8×10^{-3}	3.3×10^{-3}

to open at a sub-multiple of the flash-lamp repetition rates. For example, with the lamps flashing at 48 Hz, the Q-switch can be triggered at 1, 2, 3, 4, 6, 8, 12, 16, 24, or 48 Hz. With this approach, the average output power of the laser can vary while the peak power per pulse is maintained constant.

In the frequency-doubled mode, the laser generates 0.25 J per pulse at 0.532 μm. The Q-switched 1.064-μm output is doubled in a KD*P crystal external to the cavity in Type-II phase matching. Both the visible and the infrared laser beams will be used in active satellite-tracking experiments. This will enable us to validate our models for the wavelength dependence of atmospheric turbulence on laser beam propagation.

Figure 4 is a diagram of the optical train that couples the high-power Nd:YAG laser to the telescope. The figure shows the transmitter, the receiver, and the tracking channels. The laser transmitter channel starts at the exit of a high-power Nd:YAG laser with a linearly polarized beam approximately 11.5 mm in diameter. Exiting the laser, the beam passes through a half-wave plate that orients the electric vector of the beam in the optical train. It then passes through a beam-dividing system that splits the single laser beam into four parallel beams of equal power. The four beams enter a folded two-element refractive 2:1 beam reducer, with the resulting four-beam pattern diameter approximately 13 mm and each beam measuring about 5 mm in diameter. A half-wave plate located after the beam reducer orients the electric vector of each beam before the beams reach the calcite transmit/receive isolation polarizing beam splitter (POL B/S).

After passing through the polarizing beam splitter and fold mirror, a spherical collimator/imager mirror brings the four laser beams to a common focus at the coudé focal plane of the 1.0-m OCTL telescope. The beam is folded four times before reaching the telescope coudé focus. At the coudé focus, a spherical field mirror images the YAG laser beam waist at the telescope primary mirror. After reflecting from the field mirror and three flat-fold mirrors, a quarter-wave plate converts the four linearly polarized beams to circular polarization. The beams pass through a two-element achromatic extender lens, which effectively increases the telescope focal length by a factor of ten. Beyond the extender lens, the collimated beams propagate through the seven telescope mirrors, with the four collimated laser beams approximately 320 mm in diameter equally spaced on the telescope aperture.

For the receiver channel, the laser radiation retroreflected from the satellite and collected by the telescope is relayed through the same transmit channel optics up to the polarizing beam splitter. The circular polarization of the received beam is orthogonal to that of the transmitted beam. The return

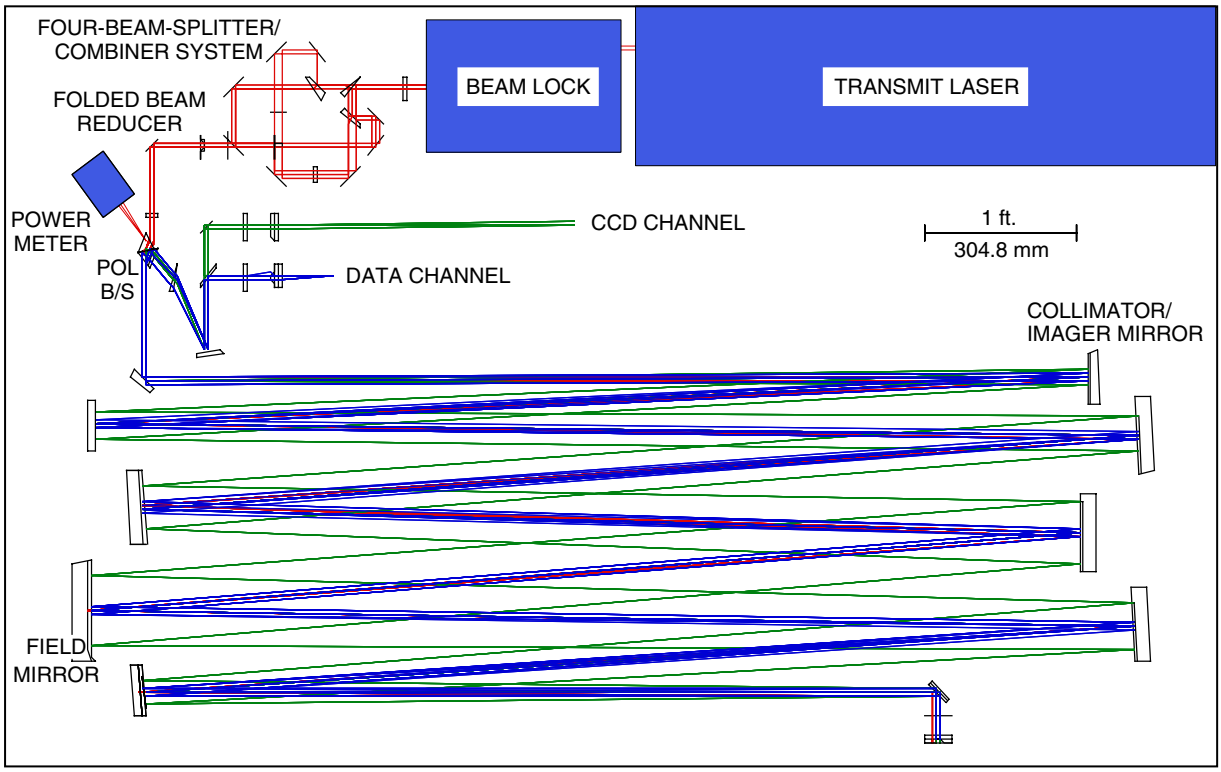

Fig. 4. Schematic of the active satellite-tracking optical train showing the transmitter, receiver, and tracking channels.

signal thus is reflected through the escape window of the calcite polarizing beam splitter. Upon exiting the calcite beam splitter, the beam passes through an anamorphic prism corrector, which compensates for the beam distortion caused by the prism effect in the polarizing beam splitter's escape optical path. It then is reflected to a non-polarizing spectral beam splitter by a single-fold mirror. Here, the laser radiation is reflected into the receiver channel, passing through a narrowband pass filter, and onto an imager lens that focuses it onto a high-speed avalanche photodiode detector. The broadband radiation reflected from the Sun-illuminated spacecraft is transmitted through the spectral beam splitter and directed into the tracking channel. Within the channel, the beam reflects off a fold mirror to an imager lens and focuses onto a charge-coupled device (CCD) detector array.

V. Adaptive Optics Enhancement of Daytime Communications Performance

Advanced signal modulation techniques combined with spectral and spatial filtering can improve the performance of the optical receiver in the presence of sky background and other broadband optical noise sources. In the pulse-position modulation (PPM) format, the slot width decreases as the PPM order increases. For a constant background source, therefore, higher-order PPM formats reduce the noise background in the signal slot. Yet, because higher-order PPM formats increase the complexity of both the transmitter and receiver electronics, increasing the PPM order is not seen as a single-point solution to improving the daytime performance of the link.

Narrowband spectral filters are loss elements in the optical train and, for a deep-space optical downlink, can require an increase in transmitted power to achieve the required link margin. Spatial filtering requires correcting wave-front aberrations caused by atmospheric turbulence. Adaptive optics techniques correct such wave-front aberrations and can achieve near-diffraction-limited imaging of the downlink signal at the receiver, and consequent reduction in the noise scattered into the receiver.

To assess the benefit of adaptive optics, we analyzed the performance of a 10-Mb/s communications system using (256-PPM, 64-PPM, and 16-PPM) modulation formats and background conditions of 0.5, 10, and 100-μW/cm^2-nm-sr incident on a 1-Å optical filter centered at 1064 nm. The wave-front correction achievable across a 1-m-aperture telescope with a deformable mirror with actuator spacings of 10 cm (n = 9), 5 cm (n = 21), and 3 cm (n = 31) was calculated assuming a Fried coherence parameter, r_o = 7 cm at 1064 nm. The actual number of actuators was n^2. We calculated the size of the field of view with 80 percent of the signal energy enclosed, and then used the result to determine the background noise power incident on the detector for each of the actuator spacing values. The noise energy in the slot then was calculated and compared for the different modulation formats. Figure 5 gives the results of this comparison for the three actuator spacings and three modulation formats. Also included in the figure are the results for a fully corrected system, i.e., one with no wave-front aberration. The results are shown for three background levels corresponding to clear sky seen from 3-km altitude [5], nominal sea-level sky radiance [6], and sunlight scattered from the telescope mirrors [6]. The figure shows that the greatest improvement (5.7 dB) is realized for the PPM-16 format when the background noise is highest. The least benefit (0.1 dB) is realized with PPM-256 when the background noise is lowest. Adaptive optics experiments planned at the OCTL will validate the results of these and other models.

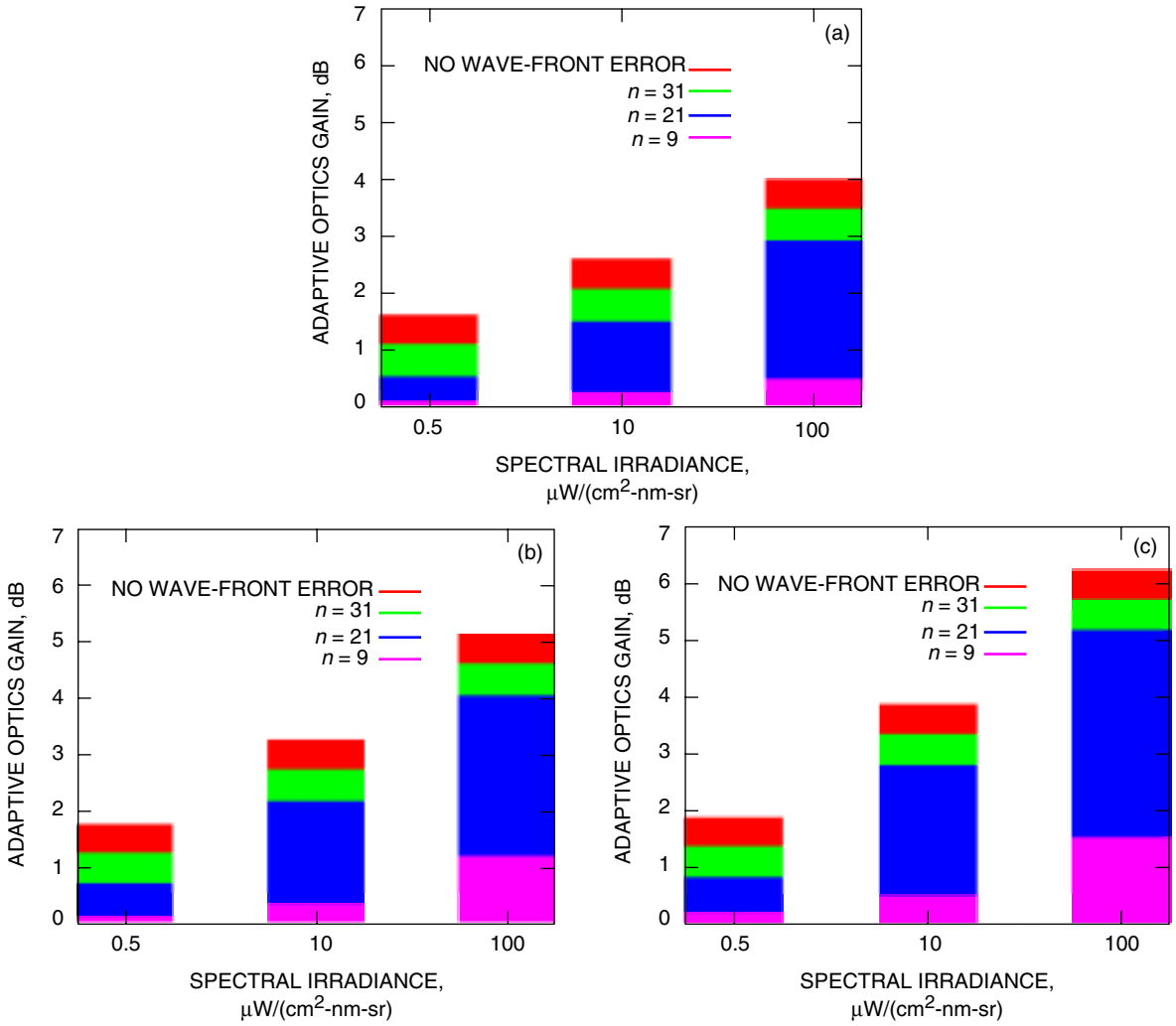

Fig. 5. Improvement in SNR for different background levels realized by implementing adaptive optics across a 1-m aperture: (a) 256-PPM, r_o = 7 cm, probability of bit error (PBE) = 0.01, (b) 64-PPM, r_o = 7 cm, PBE = 0.01, and (c) 16-PPM, r_o = 7 cm, PBE = 0.01.

VI. Strategies for Safe Ground-to-Space Laser Beam Propagation

An autonomously operated deep-space ground station network will reduce the cost of future deep-space mission support. In the U.S., laser beam propagation through the atmosphere is regulated by several government agencies and requires implementation of strategies to ensure that neither the flying public nor space assets are put at risk. To support future deep-space optical communications, OCTL researchers are developing a four-tier safety system to meet the safety requirements of these agencies [7]. The first tier, designated Tier 0, is internal to the Laboratory and is governed by the Occupational Safety and Health Administration (OSHA) with well-established and documented guidelines and procedures, which would be redundant to discuss further in this article.

Figure 6 shows the three tiers corresponding to beam propagation outside the telescope. Tiers 1 and 2 combined cover the airspace controlled by the Federal Aviation Administration (FAA). Tier 1 is designed to detect small and low-flying aircraft and covers the area ranging from the telescope dome out to a radius of 3.4 km. Tier 2 defines an ellipsoidal area around the telescope reaching 20 km at zenith and 58 km at 20-deg elevation—a region that is traveled predominantly by commercial aircraft. Lastly, regulated by the Laser Clearinghouse of the U.S. Space Command at Cheyenne Mountain, Tier 3 extends from near Earth to the ranges of geo-stationary and high elliptical-orbiting satellites.

The Laser Safety Monitoring (LSM) system under development at JPL is an integrated system that will receive and process inputs from Tiers 1 through 3 to command a beam-interrupt shutter located in the laser beam path. With the exception of Tier 3 (discussed below), the sensor for each tier is a packaged system equipped with instrumentation to scan its coverage area and its own electronics and processor to identify objects within its defined exclusion zone. When an object is detected within the exclusion zone of any one tier, the corresponding sensor is required to issue a signal that the shutter must be activated to block the path of the laser beam. In addition, since each tier operates independently, each is required to issue a signal that its detection system is running properly.

The Tier 1 sensor shown in Fig. 7 was developed by Image Labs International (ILI) and consists of a pair of long-wave infrared (LWIR) cameras to detect low-flying aircraft and other small private aircraft during both daytime and nighttime operations. The ILI system, which operates at a rate of 30 Hz with its own control system and processing algorithms, issues two outputs: (1) a +5 VDC signal when the system is running properly (0 VDC otherwise) and (2) a 0 VDC signal when an object is detected in the exclusion zone (+5 VDC otherwise).

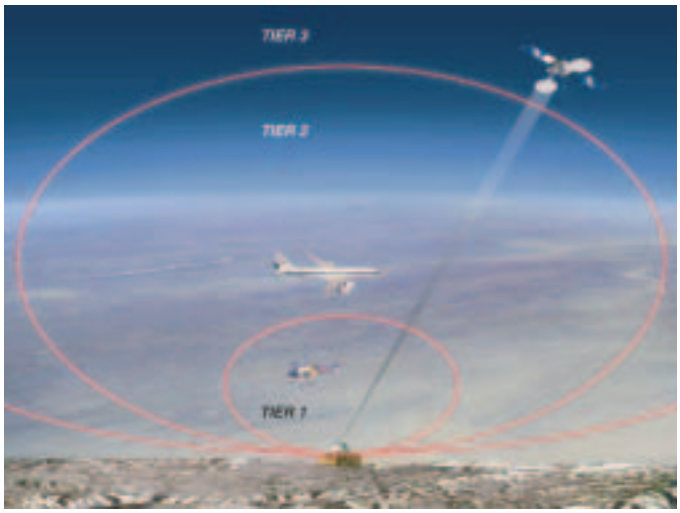

Fig. 6. Three JPL-defined safety tiers for ground-to-space laser beam propagation.

Fig. 7. Image Labs International LWIR detection system for Tier 1 aircraft avoidance.

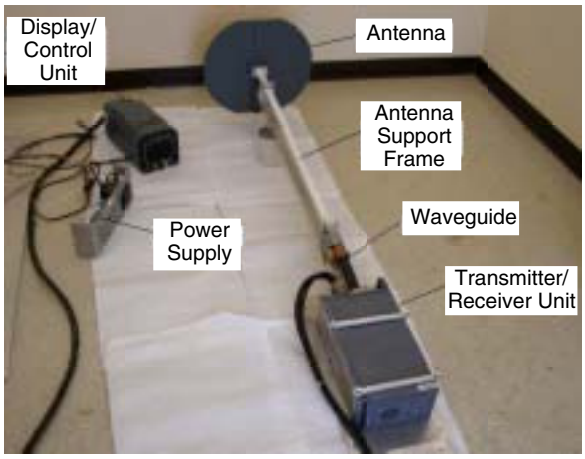

Fig. 8. JPL-modified Honeywell Primus-40 weather radar system for Tier 2 aircraft avoidance.

The Tier 2 sensor, shown in Fig. 8, uses a JPL-modified Honeywell Primus-40 weather radar system, which consists of a transmitter/receiver unit that operates at a rate of 121 Hz, a display/control module, and JPL-designed interface electronics to relay sensor status to the central data processing unit.[3] Similar to the ILI system, the modified radar system supplies two outputs: (1) a +5 VDC signal when the system is running properly (0 VDC otherwise) and (2) a +5 VDC signal when an object is detected (0 VDC otherwise). Unlike the previous two tiers, Tier 3 implements a predictive avoidance method rather than a sensor package. Laser propagation into space requires that the laser and its site be registered with the U.S. Space Command. Based on the information submitted to the Laser Clearinghouse, coordination of all laser activity may be required. Should laser operation require such coordination, the operator must provide a list of experiment times and pointing directions to the Laser Clearinghouse for approval. If an asset is deemed to be at risk, then the Clearinghouse will respond with a list of times that laser transmission is precluded.

[3] V. Garkanian, "Tier II Safety System for OCTL Station," JPL Interoffice Memorandum (internal document), Jet Propulsion Laboratory, Pasadena, California, January 2003.

Because the detection system for each tier operates independently and the sampling rates for the sensors are different, the shutter control command can be generated at different times and triggered and cleared by any or all of the three tiers. It is therefore crucial to monitor the sensor status of each tier and unify the shutter signal outputs before commanding the shutter. The JPL LSM application program not only addresses these issues but also (1) provides a unified user display for the multi-tier safety system, (2) processes supplied predictive avoidance information to evaluate whether Tier 3 object avoidance is in effect, (3) provides sole control over the shutter, and (4) records the activity of each tier to a file for future audit. The application program is Windows®-based and uses an input/output (I/O) board to output signals to activate the shutter and accept the state and shutter signals from Tiers 1 and 2 at 18,150 Hz, a rate derived by taking the least common multiple of the Tier 1 and Tier 2 operating rates. At the onset of operation, the program prompts the user for the file containing the predictive avoidance data. These data are processed internally, and the program first determines whether the times listed for unapproved laser propagation are expired or valid. If the data are valid, they will be evaluated to issue Tier 3 shutter signals at the same rate used to accept the other tier signals. The program then applies a logical OR to all tier signals to determine whether the shutter should be activated to block the laser beam path, in which case all signals are time stamped and recorded to file in addition to activating the shutter. The signals are recorded at a rate matching that of the tier system that was triggered (30 Hz for Tier 1, 121 Hz for Tier 2, and once every 30 seconds for Tier 3). Only when each tier is running properlyand no at-risk object is detected will the shutter open. Once the shutter is commanded to open, the data received from all tiers are time stamped and recorded. The user display is updated at 1 Hz to confirm to the operator that the software is executing properly. Figure 9 shows a flowchart representation of the LSM application software.

VII. Conclusion

JPL is building a research and development Optical Communications Telescope Laboratory at its Table Mountain Facility. The 1-m OCTL telescope is capable of tracking satellites as low as 250 km with great precision. Originally planned to be on site around mid-year 2002, manufacturing delays have resulted in schedule slips, pushing the period of telescope installation into the spring of 2003. We have described a series of near-term experiments for the OCTL, among which are (1) developing strategies to mitigate the effects of atmospheric scintillation on the uplink, (2) using adaptive optics techniques to improve the SNR for daytime reception at angles close to the Sun, and (3) developing safe laser propagation procedures to enable autonomous operation from remote sites. Measuring the return signal strength and frequency from actively tracked retroreflecting satellites will enable validation of models developed for the scintillation mitigation that would be achievable by multi-beam uplink transmission. The models developed from these early experiments will be further exercised in planned air-to-ground optical links. Follow-on adaptive optics experiments will allow assessment of the enhancement in receiver performance that can be achieved during daytime operation.

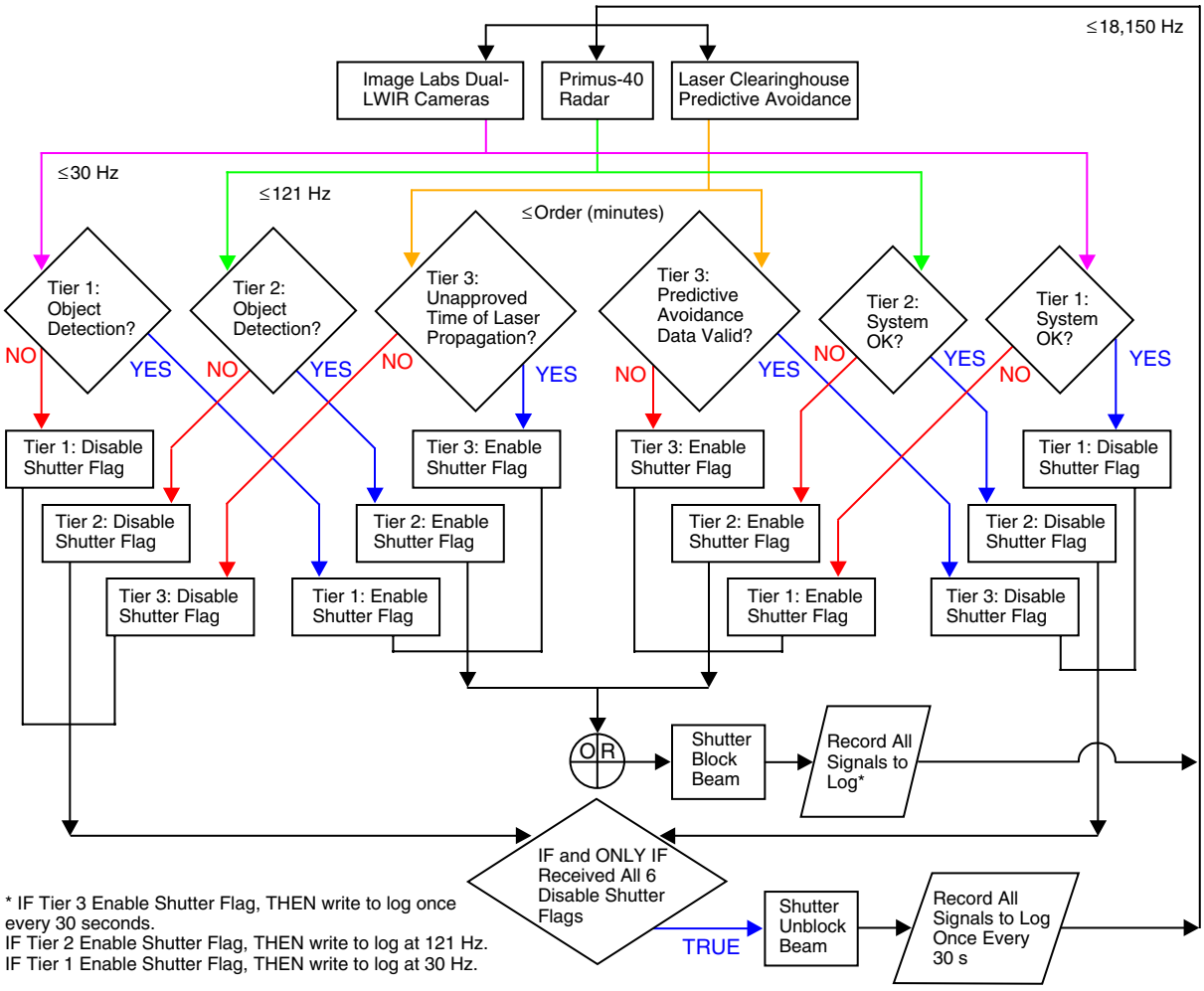

Fig. 9. LSM application software flowchart.

References

[1] http://www.uhsa.uh.edu/gov/federal/2003/fedupdate030206.html.

[2] M. Jeganathan, A. Portillo, C. Racho, S. Lee, D. Erickson, J. DePew, S. Monacos, and A. Biswas, "Lessons Learnt from the Optical Communications Demonstrator (OCD)," *SPIE Proceedings, Free-Space Laser Communications Technologies XI,* vol. 3615, pp. 23–30, January 1999.

[3] D. Erickson and K. Cowles, "Options for Daytime Monitoring of Atmospheric Visibility in Optical Communications," *The Telecommunications and Data Acquisition Progress Report 42-97, January–March 1989,* Jet Propulsion Laboratory, Pasadena, California, pp. 226–234, May 15, 1989. http://tmo.jpl.nasa.gov/tmo/progress_report/42-97/97X.PDF

[4] G. G. Ortiz, A. Portillo, S. Lee, and J. Ceniceros, "Functional Demonstration of Accelerometer-Assisted Beacon Tracking," *SPIE Proceedings, Free-Space Laser Communications Technologies XIII,* vol. 4272, p. 112, January 2001.

[5] E. E. Bell, L. Eisner, J. Young, and R. A. Oetjen, "Spectral Radiance of Sky and Terrain at Wavelengths between 1 and 20 Microns. II. Sky Measurements," *JOSA,* vol. 50, no. 12, pp. 1313–1320, December 1960.

[6] J. V. Sandusky, D. J. Hoppe, and M. J. Britcliffe, "Deep-Space Optical Reception Antenna (DSORA): Aperture Versus Quality," *The Telecommunications and Mission Operations Progress Report 42-143, July–September 2000,* Jet Propulsion Laboratory, Pasadena, California, pp. 1–11, November 15, 2000. http://tmo.jpl.nasa.gov/tmo/progress_report/42-143/143C.pdf

[7] K. E. Wilson, W. T. Roberts, V. Garkanian, F. Battle, R. Leblanc, H. Hemmati, and P. Robles, "Plan for Safe Laser Beam Propagation from the Optical Communications Telescope Laboratory," *The Interplanetary Network Progress Report 42-152, October–December 2002,* Jet Propulsion Laboratory, Pasadena, California, pp. 1–17, February 15, 2003. http://ipnpr.jpl.nasa.gov/progress_report/42-152/152G.pdf